

# Near-infrared observations of Rotating Radio Transients

N. Rea<sup>1,2\*</sup>, G. Lo Curto<sup>3</sup>, V. Testa<sup>4</sup>, G. L. Israel<sup>4</sup>, A. Possenti<sup>5</sup>, M. McLaughlin<sup>6,7</sup>,  
F. Camilo<sup>8</sup>, B.M. Gaensler<sup>9</sup>, M. Burgay<sup>5</sup>

<sup>1</sup> *Institut de Ciències de l'Espai (ICE-CSIC, IEEC), Campus UAB, Fac. de Ciències, Torre C5-parell, 2a planta, 08193 Barcelona, Spain*

<sup>2</sup> *University of Amsterdam, Astronomical Institute “Anton Pannekoek”, Postbus 94249, 1090 GE, Amsterdam, The Netherlands*

<sup>3</sup> *European Southern Observatory, Av. Alonso de Cordova 3107, Vitacura, Santiago, Chile*

<sup>4</sup> *INAF - Osservatorio Astronomico di Roma, Via Frascati 33, 00040 Monte Porzio Catone, Italy*

<sup>5</sup> *INAF - Osservatorio astronomico di Cagliari, Poggio dei Pini, Strada 54, 09012 Capoterra (CA), Italy*

<sup>6</sup> *Department of Physics, West Virginia University, Morgantown, WV 26506, USA*

<sup>7</sup> *National Radio Astronomy Observatory, Green Bank, WV 24944, USA*

<sup>8</sup> *Columbia Astrophysics Laboratory, Columbia University, New York, NY 10027, USA*

<sup>9</sup> *Sydney Institute for Astronomy, School of Physics, The University of Sydney, NSW 2006, Australia*

26 October 2018

## ABSTRACT

We report on the first near-infrared observations obtained for Rotating Radio Transients (RRATs). Using adaptive optics devices mounted on the ESO Very Large Telescope (VLT), we observed two objects of this class: RRAT J1819–1458 and RRAT J1317–5759. These observations have been performed in 2006 and 2008, in the J, H and  $K_s$  bands. We found no candidate infrared counterpart to RRAT J1317–5759 down to a limiting magnitude of  $K_s \sim 21$ . On the other hand, we found a possible candidate counterpart for RRAT J1819–1458 having a magnitude of  $K_s = 20.96 \pm 0.10$ . In particular, this is the only source within a  $1\sigma$  error circle around the source’s accurate X-ray position, although given the crowded field we cannot exclude that this is due to a chance coincidence. The infrared flux of the putative counterpart to the highly magnetic RRAT J1819–1458 is higher than expected from a normal radio pulsar, but consistent with that seen from magnetars. We also searched for the near-infrared counterpart to the X-ray diffuse emission recently discovered around RRAT J1819–1458, but we did not detect this component in the near-infrared band. We discuss the luminosity of the putative counterpart to RRAT J1819–1458 in comparison with the near-infrared emission of all isolated neutron stars detected to date in this band (5 pulsars and 7 magnetars).

**Key words:** stars: pulsars: general — pulsar: individual: RRAT J1819–1458, RRAT J1317–5759

## 1 INTRODUCTION

Rotating Radio Transients (RRATs) are a recently discovered class of neutron stars (McLaughlin et al. 2006, 2009; Keane et al. 2010) characterized by dispersed radio bursts with flux densities (at a wavelength of 20 cm) ranging from  $\sim 100$  mJy to 4 Jy, durations from 2 and 30 ms, and average intervals between repetition from 4 minutes to 3 hours. Periodicities have been inferred through the study of arrival times of these bursts, ranging between 0.1–7 s. The timing solutions derived from the radio bursts, i.e. their periods and period derivatives, indicate that they are neutron stars (McLaughlin et al. 2006, 2009).

The detection of such sources is rather difficult, mainly due to the very tiny duty cycle of their radio bursts (0.1–1 s of radio emission per day). Detailed population studies show that there may be more RRATs than canonical rotational powered radio pulsars in our Galaxy (McLaughlin et al. 2006, 2009; Keane & Kramer 2008).

Determining the nature of the emission from these objects and how many RRATs are present in our Galaxy is of paramount importance for pulsar emission theories, as well as for neutron star population studies. Up to now many hypotheses on the nature of these objects have been put forward, based on the comparison with the radio pulsar class: e.g. that the RRATs may be neutron stars near the radio “death line” (Zhang et al. 2006), or that the sporadicity of the RRATs is due to the presence of a circumstellar as-

\* Ramon y Cajal Research Fellow; rea@ieec.uab.es.

RRAT J1819-1458					
Date	Filter	FWHM(pix)	Exp.Time	Mag. Lim.(3 $\sigma$ )	zero point
2006 Jun. 26	K <sub>s</sub>	2.9	2280	21.4	22.52±0.06
2006 Jun. 26	J	5.0	1620	22.8	23.27±0.18
2006 Jun. 28	H	3.2	1620	21.8	23.12±0.07
2006 Jul. 21	H	3.1	1800	22.4	23.43±0.07
2006 Jul. 31	J	10.0	1800	22.9	23.67±0.06
2008 Jul. 18	K <sub>s</sub>	4.0	1080	20.7	22.40±0.08
RRAT J1317-5759					
Filter	Date	FWHM(pix)	Exp.Time	Mag. Lim.(3 $\sigma$ )	zero point
2006 Apr. 02	K <sub>s</sub>	3.2	2280	20.90	22.48±0.06
2006 Apr. 02	J	6.2	2520	22.70	23.14±0.07
2006 Apr. 27	H	3.9	1320	20.90	22.55±0.06
2006 Apr. 28	H	3.9	2280	22.80	23.06±0.06

**Table 1.** Summary of the ESO-VLT observations of RRAT J1819–1458 and RRAT J1317–5759. The NACO pixel size corresponds to 0.027".

teroid belt (Cordes & Shannon 2008; Li 2006) or a radiation belt such as seen in planetary magnetospheres (Luo & Melrose 2007). Note that, even though they are all characterized by a similar radio bursting activity, RRATs might be an inhomogeneous group of sources, comprising neutron stars belonging to different classes. Interesting possibilities are the connection with i) the transient magnetars, given the recent radio detection during their outbursts (Camilo et al. 2006, 2007); ii) with the X-ray Dim Isolated Neutron Stars (XDINSs; Haberl 2007; van Kerkwijk & Kaplan 2007; Popov 2006), given the thermal X-ray emission discovered for RRAT J1819–1458, being so far the most magnetic RRAT (Reynolds et al. 2006; McLaughlin et al. 2007); and iii) with the radio pulsars showing thermal X-ray emission, such as PSR B0656+14, which has been argued to be a close RRAT (Weltevredre et al. 2006).

Optical and infrared counterparts have been identified so far only for ten rotational powered radio pulsars ( $V \sim 26$ ; see Mignani et al. 2009 for a recent review), four XDINSs ( $V \sim 25$ ; van Kerkwijk & Kaplan 2007), and seven magnetars ( $K_s \sim 20$ ; Israel et al. 2004; Testa et al. 2008; Mereghetti 2008). Despite being all isolated neutron stars, their optical and infrared emission has distinctive properties depending on the source class. Very little is known about a possible optical or infrared component in the emission of RRATs, beside the non-detection of optical bursting emission (Dhillon et al. 2006). The detection and characterization of the nature of the putative infrared emission of RRATs is a crucial help to assess their relation with any of the aforementioned neutron star classes.

We report in this paper on the first infrared observations of RRATs, in particular we study two sources of this class having a relatively good positional accuracy: RRAT J1819–1458 and RRAT J1317–5759<sup>1</sup>. The paper is structured as

follows: in §2 we report on the observations and data analysis, in §3 we show the results of our infrared study, and discussion follows (§4).

## 2 OBSERVATIONS, CALIBRATIONS AND ANALYSIS

Observations have been obtained during years 2006 and 2008, with the ESO VLT-UT4 Yepun, equipped with the adaptive optics near-infrared camera NACO (NAOS/CONICA) in three filters: J ( $\lambda = 12650\text{\AA}$ , FWHM = 2500  $\text{\AA}$ ), H ( $\lambda = 16600\text{\AA}$ , FWHM = 3300  $\text{\AA}$ ), and K<sub>s</sub> ( $\lambda = 21800\text{\AA}$ , FWHM = 3500  $\text{\AA}$ ). In some cases the objects have been observed in more than one epoch, as summarized in the Tab. 1. All the observations have been performed with airmass between 1.0-1.3, a seeing  $<1''5$ , and using natural guide stars for the adaptive optic system.

The data were reduced using the standard strategies for near-infrared data reduction. Flat fielding was done via internal lamp flats. Sky emission has been computed using IRAF<sup>2</sup> on the dithered images and then subtracted on each image before de-jittering. We used the *eclipse*<sup>3</sup> package to co-add the images. Every pointing is the co-addition of three images of 40s - 60s each, depending on the filter. This co-addition is performed by the computer on board the instrument, and we obtain only one image per dithering position. Fig. 1 and Fig. 2 show finding charts in the K<sub>s</sub> band for the two studied RRATs, with the source positions highlighted.

We first reduced the images with the IRAF version of *daophot*, using the PSF fitting algorithm. Aperture photometry was also performed using an aperture diameter twice the measured FWHM. Aperture and PSF photometries have been compared by applying aperture corrections using the

<sup>1</sup> Within our ESO-VLT observing campaign, we also took observations of RRAT J1913+1333. However during the submission of this paper, we became aware that the published position of this RRAT was off by  $\sim 3'$ , hence the correct position (McLaughlin et al. 2009) lies outside the VLT-NACO field of view of our observations.

<sup>2</sup> IRAF is distributed by the National Optical Astronomy Observatories, which are operated by the Association of Universities for Research in Astronomy Inc., under cooperative agreement with the National Science Foundation.

<sup>3</sup> www.eso.org/eclipse

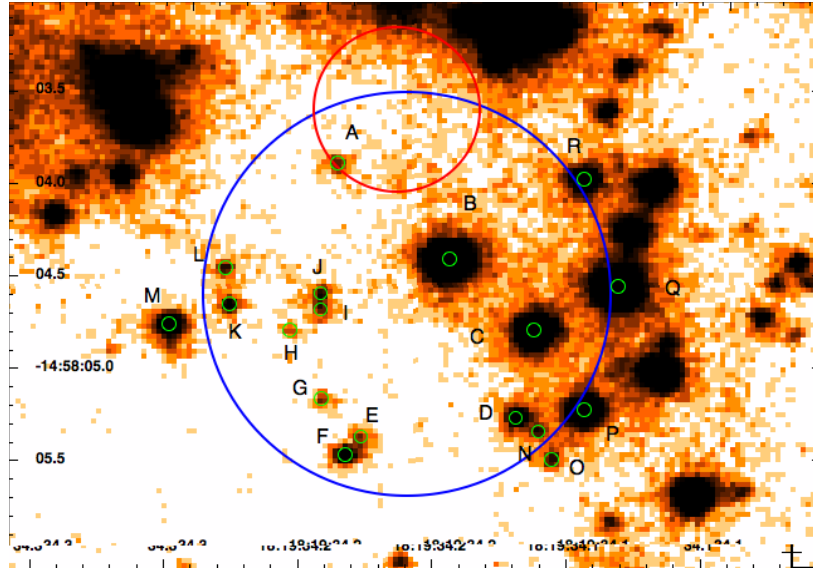


**Figure 1.** RRAT J1819–1458 : ESO–VLT  $K_s$ -band image of the June 2006 observation. The  $1\sigma$  error circle around the new X-ray position of the RRAT is marked ( $0''.45$ ; Rea et al. 2009a). Small circles (see also Tab. 2) show the position of the stars close or near the RRAT  $2\sigma$  old X-ray position ( $1''$ ; Reynolds et al. 2006). All positional errors are weighted with the uncertainty in the NACO astrometry (see text for details), and the coordinate grid in RA and Dec (J2000) is overplotted. North is on top and East is left.

Source		J band		H band		K <sub>s</sub> band		
ID	RA (h m s)	Dec (d m s)	2006-06-26	2006-07-31	2006-06-28	2006-07-21	2006-06-26	2008-07-18
A	18 19 34.20	-14 58 03.9	-	-	-	-	20.96±0.10	-
B	18 19 34.15	-14 58 04.4	21.05±0.19	21.03±0.07	18.56±0.07	18.52±0.06	17.89±0.06	17.95±0.08
C	18 19 34.12	-14 58 04.8	22.52±0.21	22.89±0.12	19.43±0.09	19.49±0.06	18.49±0.07	18.47±0.09
D	18 19 34.13	-14 58 05.3	22.69±0.21	22.40±0.10	20.50±0.10	20.51±0.07	19.99±0.08	20.10±0.10
E	18 19 34.19	-14 58 05.4	-	-	-	-	20.94±0.10	-
F	18 19 34.19	-14 58 05.5	-	-	21.83±0.20	21.36±0.08	20.13±0.08	20.35±0.10
G	18 19 34.20	-14 58 05.2	-	-	-	22.49±0.11	20.87±0.10	-
H	18 19 34.21	-14 58 04.8	-	-	-	-	21.09±0.11	-
I	18 19 34.20	-14 58 04.7	-	-	-	-	20.97±0.10	-
J	18 19 34.20	-14 58 04.6	-	-	-	21.86±0.09	20.86±0.10	-
K	18 19 34.24	-14 58 04.7	-	-	21.24±0.13	21.10±0.08	20.61±0.09	20.59±0.11
L	18 19 34.24	-14 58 04.5	-	-	-	-	20.64±0.09	-
M*	18 19 34.26	-14 58 04.8	23.10±0.22	-	20.19±0.10	20.20±0.07	19.47±0.07	19.45±0.09
N	18 19 34.12	-14 58 05.3	-	-	-	-	20.90±0.10	-
O	18 19 34.12	-14 58 05.5	-	-	21.38±0.14	21.59±0.08	20.83±0.10	-
P	18 19 34.10	-14 58 05.2	21.89±0.19	21.82±0.08	19.37±0.07	19.36±0.06	18.89±0.07	18.87±0.09
Q	18 19 34.09	-14 58 04.6	21.56±0.19	21.55±0.08	18.74±0.07	18.76±0.06	17.90±0.06	17.82±0.08
R	18 19 34.10	-14 58 04.0	22.80±0.21	22.59±0.10	19.87±0.09	19.91±0.07	19.37±0.07	19.20±0.09

**Table 2.** Magnitudes of the sources close to RRAT J1819–1458 (see also Fig. 1). RA and Dec refer to J2000. \* Possible extended source.

IRAF *daogrow* algorithm, which calculates the aperture correction extrapolating to an aperture at infinity.

Furthermore, due to the crowding of the fields, we checked the photometry via a deconvolution code: DECPHOT (Gillon et al. 2006, 2007; Magain et al. 2007), based on the "MCS" algorithm (Magain, Courbin & Sohy

1998). The basic idea of the MCS code, is that of "partial" deconvolution: the data are deconvolved to a higher resolution, but at a level that the Nyquist criterium for a correct sampling was satisfied. This resulted in excellent photometric and astrometric accuracy. At variance with the standard MCS method, the code by Gillon et al. (2006, 2007) is faster,

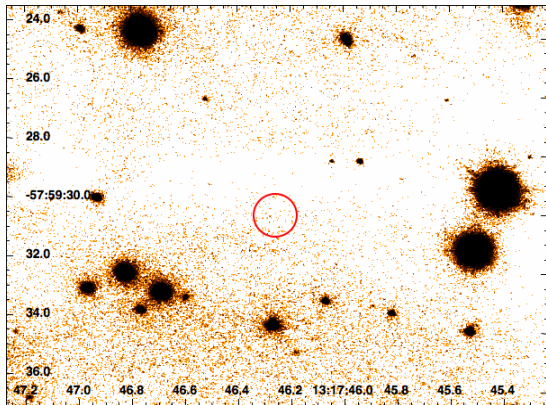


**Figure 2.** RRAT J1317–5759: ESO–VLT  $K_s$ -band image with the  $1\sigma$  error circle around the refined position (see text for details). The coordinate grid in RA and Dec (J2000) is overplotted. North is on top and East is left.

determines the PSF “on the fly” and fits the sky background. We report hereafter the photometry delivered by this code, which was compatible, for the most isolated objects, with the photometry from the `imexam` task of IRAF and with `daophot`.

Calibrations have been performed using photometric standard stars observed within 4 hours from our target. The calibrated catalogs were then matched for each filter, and compared to verify the self-consistency of the calibrations. Small differences in the calibrations have been found between the J, H, and  $K_s$  images in different epochs, in this case the best quality epoch has been chosen as reference and the magnitudes of the other epoch reported to it, for each source respectively.

Further check with the 2MASS catalog has been performed but unfortunately the 2MASS objects present on the images were saturated or at the saturation limit and thus the zero point check with the 2MASS was not constructive. Furthermore, the 2MASS catalog was built from images with a  $2''$  pixel size, and in many cases the measured magnitudes correspond to blended objects which are, instead, resolved in our higher resolution images. The calibrated catalogs for the single filters were then matched to produce a final master catalog.

In all cases, astrometric calibration was performed using 2MASS stars as reference, yielding an average uncertainty of  $\sim 0''.33$  ( $1\sigma$  confidence level), after accounting for the intrinsic astrometric accuracy of 2MASS and the r.m.s. of the astrometric fits.

## 3 RESULTS

### 3.1 RRAT J1819–1458

This is the most prolific radio burster among the RRAT class, with a magnetar-like dipolar magnetic field at sur-

face of  $B \sim 5 \times 10^{13}$  Gauss, and a spin period of  $\sim 4.26$  s (McLaughlin et al. 2006; Lyne et al. 2009). It is so far the only member of the class for which X-ray emission has been discovered (Reynolds et al. 2006; McLaughlin et al. 2007), with a luminosity of  $L_X = 4 \times 10^{33} \text{erg s}^{-1}$  (assuming a distance of 3.6 kpc). Diffuse X-ray emission has been recently reported for RRAT J1819–1458 with a luminosity of  $\sim 10^{32} \text{erg s}^{-1}$  and extending until  $\sim 13''$  from the source (Rea et al. 2009a). Furthermore, the RRAT error circle has been recently refined performing a bore-site correction of a new *Chandra* observation which were tied to the 2MASS field using a field star present in both the X-ray and infrared images. This resulted in an accurate position of RA 18:19:34.173, Dec -14:58:03.57 (J2000) with a  $1\sigma$  error of  $\sim 0''.3$  (Rea et al. 2009a).

We took observations in the three standard near-infrared bands (J, H and  $K_s$ ), and in two epochs per filter (see Tab. 1). These resulted in the identification of a possible candidate near-infrared counterpart to RRAT J1819–1458, the only source within the  $1\sigma$  X-ray positional error circle (our source A; see Fig. 1 and Tab. 2; note that we took into account the astrometric error reported in §2, inferring a final  $1\sigma$  error circle of  $0''.45$ ). Although a few other sources lies close to RRAT J1819–1458, in particular if we enlarge the X-ray positional error circle to e.g. 90%, they are all rather bright objects, not compatible with the expected magnitudes from an isolated neutron star of any kind.

Within the limiting magnitude of our deepest exposure,  $K_s = 21.4$  (see Tab. 1), we significantly detected 380 sources within the calibrated NACO field of  $25'' \times 22''$ , which means an average of 1 source on an area of  $1''.45^2$ . Given such a crowded region we cannot exclude that the identification of source A as a possible counterpart through its proximity to RRAT J1819–1458’s X-ray position might be due to a chance coincidence, the probability of which is  $\sim 43\%$ . However, as a further selection criteria, assuming that an isolated neutron star at 3.6 kpc is not expected to have a magnitude  $< 19$  (which is the brightest K magnitude observed in an isolated neutron star, namely for SGR 0501+4561 and SGR 1806–20; Levan et al. 2010 in prep.; Israel et al. 2005), we are then left with 115 sources in the field responding to such selection, hence the probability of having in coincidence with the X-ray position a source with a magnitude expected for a possible counterpart is  $\sim 14\%$ .

The source is very faint and not visible in H and J bands within our limiting magnitudes (see Tab. 2). We detect the source only in our deepest  $K_{rms}$  image on June 2006, however no variability can be claimed since the following epoch was not deep enough to detect such a faint source. We did not find any J, H and  $K_s$  variability for the objects close to our target, both investigating different frames of a single observation, and comparing the several epochs. In Fig. 3 we show the color-magnitude and color-color diagrams for all sources in the field of RRAT J1819–1458. We did not find any source with peculiar colors. We over-plot the limits we have for our candidate counterpart (source A), which unfortunately was detected only in the  $K_s$  band, hence we have only limits on its colors, namely  $J-K_s > 1.94$  and  $H-K_s > 1.44$ . If source A is indeed the counterpart to RRAT J1819–1458, then its  $K_s$  luminosity would be  $L_{NIR} = 1.62 \times 10^{30} \text{erg s}^{-1}$  (assuming a 3.6 kpc distance;

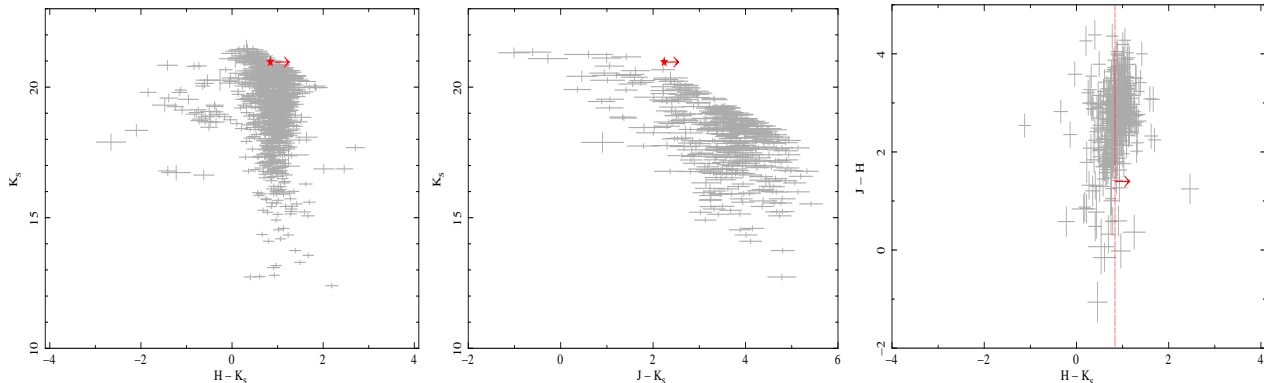


**Figure 3.** From left to right: color-magnitude ( $H-K_s, K_s$ ;  $J-K_s, K_s$ ) and color-color diagrams ( $J-K_s, H-K_s$ ) of the VLT–NACO imaged area of RRAT J1819–1458 taken in year 2006 (see also Fig. 1 and Tab. 2). The star and vertical line are relative to the limits we have for our candidate counterpart, source A.

see also Tab. 3), while if it is not, the  $3\sigma$  upper limit we derived corresponds to  $L_{\text{NIR}} < 1.51 \times 10^{30} \text{ erg s}^{-1}$ .

Furthermore, we searched for the possible near-infrared counterpart to the X-ray diffuse emission discovered around RRAT J1819–1458, removing all the sources in the field on the basis of their fitted PSF. We did not find any extended emission down to a limiting  $K_s$  surface brightness of  $> 18.5 \text{ mag/arcsec}^2$  (at a  $3\sigma$  confidence level).

### 3.2 RRAT J1317–5759

With a period of  $\sim 2.64 \text{ s}$  and a magnetic field of  $\sim 5 \times 10^{12} \text{ Gauss}$ , this RRAT has timing properties similar to many canonical radio pulsars (McLaughlin et al. 2006, 2009). The source position has been refined through radio timing analysis of the bursts: RA 13:17:46.26, Dec -57:59:30.32 (J2000) with a  $1\sigma$  error of  $0''.57$  (McLaughlin et al. 2009). X-ray observations resulted in a luminosity upper limit on its X-ray counterpart of  $L_X < 7.5 \times 10^{32} \text{ erg s}^{-1}$  (assuming a distance of 3.2 kpc; Rea & McLaughlin 2008).

We observed this object using three infrared bands ( $J, H, K_s$ ). No infrared counterpart has been detected, with limiting magnitudes reported in Tab. 1, and a  $3\sigma$  upper limit on the  $K_s$  luminosity of  $L_{\text{NIR}} < 1.3 \times 10^{30} \text{ erg s}^{-1}$ . We show in Fig. 2 the  $K_s$  finding chart around RRAT J1317–5759’s radio timing position.

## 4 DISCUSSION

Optical counterparts have been identified so far only for ten rotational powered radio pulsars, and only five of them were observed in the infrared band (see Mignani et al. 2009 for a recent review). The radio pulsars’ infrared/optical emission depends mainly on the pulsar age: young objects show pure magnetospheric emission, middle-aged ones appear to have composite spectra with an additional thermal component most probably arising from the cooling neutron star surface, while for older objects there is more confusion, but on average there is evidence for a dominant magnetospheric

component (Mignani et al. 2001; Zharikov et al. 2004).

The situation is more favorable in the case of XDINS. Four XDINSs have secure optical identifications ( $V \sim 25$ ; van Kerkwijk & Kaplan 2007), with a thermal optical emission which exceeds by a factor of  $\sim 10$  the extrapolation of their blackbody-like soft X-ray spectrum. This suggests that the thermal component responsible for the optical emission arises from a cooler and larger area, with respect to their thermal X-ray emission. None of them have been detected in the infrared band yet (Lo Curto et al. 2007).

The neutron star infrared zoo, has been joined some years ago by the magnetars. In particular, observations from large telescopes such as i.e. ESO, Gemini, CFHT, and Keck, led to the discovery of faint ( $K_s \sim 20$ ) and, in some cases variable, infrared counterparts for many magnetars (see Tab. 3 for a complete list, and also Israel et al. 2004; Testa et al. 2008; Mereghetti 2008). It is not yet clear whether infrared emission in magnetars arise from reprocessed X-ray emission via a fossil disk around the neutron star (Chatterjee et al. 2000; Perna et al. 2000), or of magnetospheric origin (Beloborodov & Thompson 2007), but it is certainly true that with respect to normal radio pulsars, their infrared emission is much more efficient (see also below and Fig. 4). Other crucial peculiarities of magnetars’ infrared emission are their strange infrared colors, usually very red with respect to their field stars (see e.g. Israel et al. 2004).

We report in this paper on the first infrared observations of RRATs, performed using the NACO camera on the ESO-VLT (see §2). We found that among the two studied RRATs, RRAT J1819–1458 and RRAT J1317–5759, only the former has a candidate infrared counterpart (see Fig. 1) within our limiting magnitudes (see Tab. 1). Unfortunately, we could detect the possible counterpart only in one  $K_s$  pointing (the deepest we had), with a magnitude of  $K_s = 20.96 \pm 0.10$ , hence we have no handle on the colors of this source because our  $J$  and  $H$  observations were not deep enough (see Fig. 3 for the limits on its color). On the other hand we have also no handle on the possible variability of this infrared counterpart (a behavior typical of magnetar infrared emission; Israel et al. 2002; Rea et al. 2004; Israel et al. 2009),

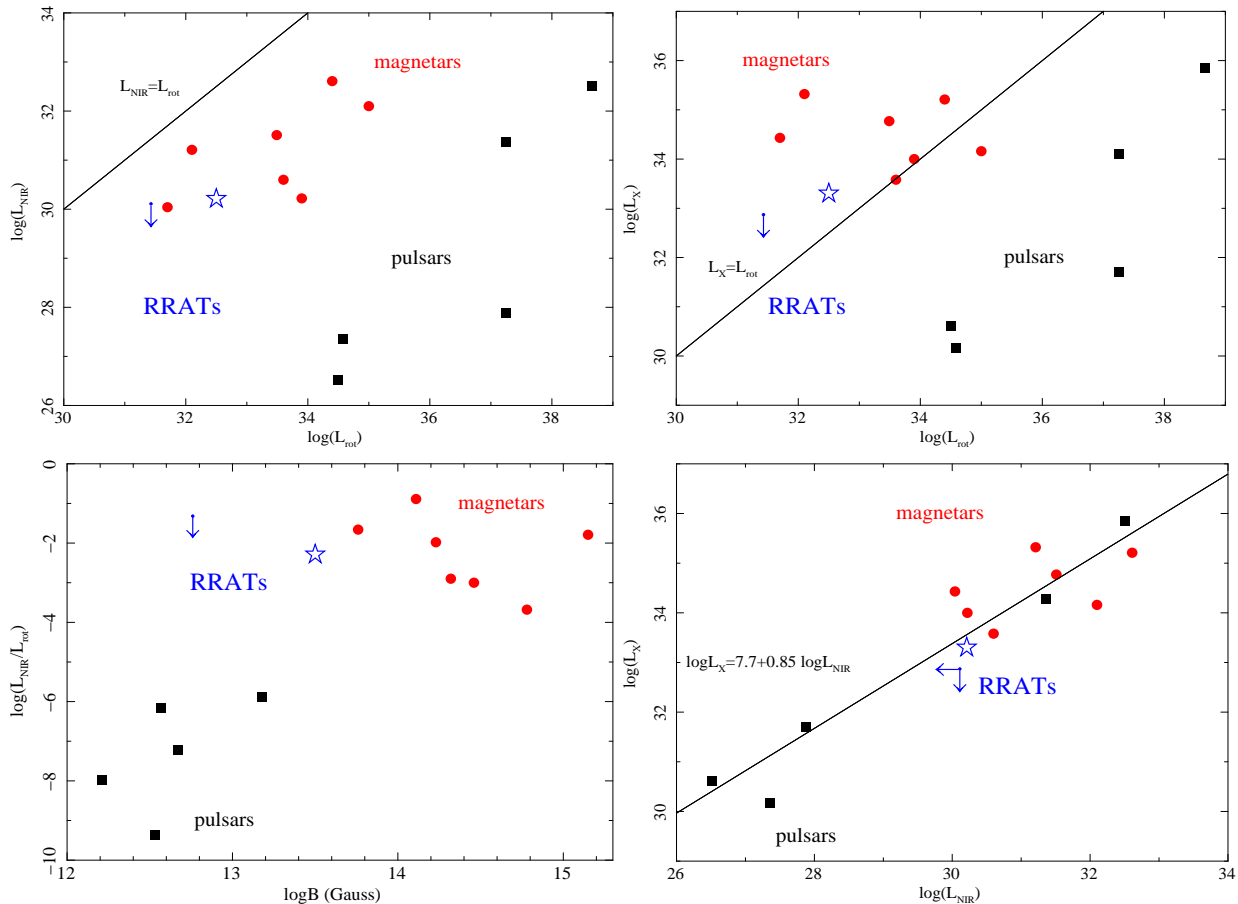


**Figure 4.** Squares, circles and the star indicate rotation-powered pulsars, magnetars, and RRAT J1819–1458, respectively, while the arrow shows RRAT J1317–5759’s upper limit (see also Tab. 3). *Top panels:* infrared and X-ray luminosities as a function of the rotational luminosity (solid lines represent  $L_{\text{NIR}}=L_{\text{rot}}$  and  $L_{\text{X}}=L_{\text{rot}}$ , respectively). *Bottom panels:* on the left we report on the infrared and rotational luminosity ratio ( $L_{\text{NIR}}/L_{\text{rot}}$ ) versus the pulsar magnetic field, while on the right-side we show the X-ray versus the infrared luminosities. The solid line here represents the fit to the data (see text for details). For all the objects  $L_{\text{NIR}}$  and  $L_{\text{X}}$  have been computed in the  $K_{\text{s}}$  and 1-10 keV bands, respectively. Errors on the source distances are not taken into account in the luminosity uncertainties.

this is why we consider it as a candidate counterpart which needs to be confirmed with further data.

With a magnitude of  $K_{\text{s}} = 20.4$  (after correcting for the extinction in the  $K_{\text{s}}$ -band derived from the X-ray absorption value  $N_{\text{H}} \sim 9 \times 10^{21} \text{ cm}^2$ ; Predehl & Smith 1995; Cardelli, Clayton & Mathis 1989), our candidate source A has a  $K_{\text{s}}$  flux density of  $F_{K_{\text{s}}} \sim 4.6 \times 10^{-29} \text{ erg s}^{-1} \text{ cm}^{-2} \text{ Hz}^{-1}$ . If confirmed, this relatively bright infrared emission strengthens the connection of RRAT J1819–1458 with the magnetar class. In particular, the intensity of its candidate counterpart would place it well among the magnetar luminosities compared with those of normal pulsars. As for the magnetars, the luminosity of this possible counterpart, lies above the extrapolation of the blackbody modelling its X-ray emission (McLaughlin et al. 2007). In Tab. 3 and Fig. 4 we computed the near-infrared luminosities ( $L_{\text{NIR}}$ ) in the  $K_{\text{s}}$  band of all isolated neutron stars detected at such wavelength (namely 5 radio pulsars and 7 magnetars). Furthermore, we calculated their X-ray luminosities in the 1-10 keV band<sup>4</sup> taking

care of choosing X-ray observations as close as possible to the date of the near-infrared ones, crucial for most of the magnetars which show variable emission in both such energy bands. However, given the non-exact simultaneity of the X-ray and near-infrared observations this luminosity comparison should be taken with the due uncertainty.

In Fig. 4 (top panels) we plot the infrared and X-ray luminosities of pulsars, magnetars and the two RRATs studied in this paper, as a function of their rotational energies (see also Tab. 3). It is clear that while the rotational energy is not at all sufficient to power magnetars’ and RRAT J1819–1458 X-ray emission, it might well suffice to be the reservoir for their infrared luminosity, as the radio pulsar case. However, even if powered by a similar mechanism, the efficiency of magnetars in converting rotational power in infrared luminosity, is much higher than normal radio pulsars, possibly due to their high magnetic fields (see also Mignani et al. 2007, 2009; Zane et al. 2008). This is particularly clear in

<sup>4</sup> We used for all magnetars the fluxes resulting from a spectral fit with a resonant cyclotron scattering model or two blackbodies

(Rea et al. 2008, 2009b), with the aim of not overestimating the  $N_{\text{H}}$  values, which would have spuriously produced overestimated X-ray luminosities.

Source	d(kpc)	$\log(L_{\text{rot}})$	$\log(L_{\text{NIR}})$	$\log(L_{\text{X}})$	$\log(B)$	Age $\tau$ (kyr)	Refs.
Crab	1.7	38.66	32.51	35.85	12.57	1.24	1,2,3
PSR 1509–58	5.2	37.25	31.36	34.28	13.18	154	4,5,6
Vela	0.3	37.25	27.88	31.70	12.53	11.3	7,8,9,10
PSR 0656+14	0.3	34.58	27.36	30.16	12.67	111	11,12,13,14
Geminga	0.16	34.50	26.51	30.62	12.21	342	11,15,16
1E 1547–5408*	9.0	35.00	32.10	34.16	14.32	1.41	17,18,19
SGR 1806–20*	8.7	34.40	32.61	35.21	15.15	0.22	20,21,22
1E 1048–5937*	3.0	33.90	30.22	34.00	14.78	2.68	23,24,25
XTE 1810–197*	4.0	33.60	30.60	33.58	14.46	1.13	26,27
SGR 0501+4516*	5.0	33.49	31.51	34.77	14.23	1.32	28,29
4U 0142+61*	5.0	32.10	31.21	35.32	14.11	67.7	30,31
1E 2259+586*	3.0	31.70	30.04	34.43	13.76	228	32,33,34,35
RRAT J1819–1458	3.6	32.50	30.21 (<30.18)	33.30	13.50	120	this work, 36, 37
RRAT J1317–5759	3.2	31.43	<30.11	<32.87	12.76	3330	this work, 36, 38

**Table 3.** Characteristics of pulsars and magnetars detected in the  $K_s$  near-infrared band, compared to the candidate infrared counterpart to RRAT J1819–1458 and RRAT J1317–5759. Luminosities are in units of  $\text{ergs}^{-1}$ . The latter are calculated in the  $K_s$ -band and in the 1–10 keV energy range for  $L_{\text{NIR}}$  and  $L_{\text{X}}$ , respectively. The magnetic field values (B) are reported in Gauss. \* Variable in the X-ray and NIR bands, not necessarily in a correlated fashion. (1) Sollerman (2003); (2) Sollerman et al. (2000); (3) Weisskopf et al. (2000); (4) Kaplan & Moon (2006); (5) Gaensler et al. (1999); (6) DeLaney et al. (2006); (7) Shibanov et al. (2003); (8) Dodson et al. (2003); (9) Mignani et al. (2003); (10) Pavlov et al. (2001); (11) Koptsevich et al. (2001); (12) Briskin et al. (2003); (13) Pavlov et al. (1997); (14) Shearer et al. (1997) (15) Caraveo et al. (1996); (16) Kargaltsev et al. (2005); (17) Israel et al. (2009); (18) Camilo et al. (2007); (19) Bernardini et al. (2010 in prep); (20) Israel et al. (2005); (21) Bibby et al. (2008) (22) Eikenberry et al. (2004); (23) Wang & Chakrabarty (2002); (24) Mereghetti et al. (2004); (25) Gaensler et al. (2005); (26) Israel et al. (2003); (27) Rea et al. (2004); (28) Levan et al. (2010 in prep); (29) Rea et al. (2009b); (30) Hulleman et al. (2004); (31) Rea et al. (2007); (32) Hulleman et al. (2001); (33) Kothes et al. (2002); (34) Woods et al. (2004); (35) Tian, Leahy & Li 2010; (36) McLaughlin et al. (2006); (37) McLaughlin et al. (2007); (38) Rea & McLaughlin (2008).

Fig. 4 (bottom-left panel), where we see how this efficiency is much higher for highly magnetic sources (as RRAT J1819–1458).

Pulsars detected in the near-infrared band are also observed as X-ray emitters: this is not only due to the trivial conclusion of being the closest, hence the most favorable for detecting their faint multi-band emission, but it is also an intrinsic connection. In particular, young objects as these particular pulsars, present more powerful magnetospheric emission, responsible for both the near-infrared and X-ray emission, which of course combined with their close distances, make them visible in both bands. Comparing the near infrared and X-ray luminosity of all isolated neutron stars detected in both these bands, we found an intriguing correlation (see Fig. 4 bottom-right panel):  $\log(L_{\text{X}}) = 7.7 \pm 2.8 + (0.85 \pm 0.09) \times \log(L_{\text{NIR}})$ . This empirical fit resulted in a  $\chi^2 = 1.3$ , with the magnetars having the largest spread over the model. This relation might be used to have a very rough estimate of the infrared luminosity of a known or new isolated neutron star, however, given the large errors in the distances (which have not been taken into account in the fit), this relation should be used with the due uncertainty.

In this picture, the  $K_s$  magnitude of our proposed candidate counterpart to RRAT J1819–1458 (source A) is too bright to be the counterpart of a normal radio pulsar, given its low rotational power, while it is well in line with the values observed for magnetars (see Fig. 4 top and bottom-left panels). This would represent only one among a series of other properties which connects this RRAT to the magnetar class, as its inferred dipolar B field ( $5 \times 10^{13}$  Gauss), its bright

X-ray emission with respect to other RRATs (McLaughlin et al. 2007; Rea & McLaughlin 2008; Kaplan et al. 2009), as well as the presence of a diffuse X-ray nebula proposed to be powered by the magnetic energy (Rea et al. 2009a).

## 5 CONCLUSION

Near-infrared observations of RRAT J1819–1458 and RRAT J1317–5759 resulted in a possible candidate counterpart for the former ( $K_s = 20.96 \pm 0.10$ ), while no infrared counterpart was detected for the latter (within the limiting magnitudes reported in Tab. 1). However, the proposed counterpart to RRAT J1819–1458 needs further confirmation due to the relatively high chance coincidence probability. Studying the near-infrared and X-ray luminosities of all isolated neutron stars detected in the  $K_s$ -band, with respect to other characteristics such as the rotational luminosity and the magnetic field, we show that the rotational energy may well be the reservoir of the magnetars and RRAT J1819–1458 infrared emission. However, in this picture the efficiency of converting rotational energy in near-infrared luminosity should be necessarily higher for highly magnetic sources.

Based on observations collected at the European Southern Observatory, Paranal, Chile under programs ID: 077.D-0395(A), 077.D-0395(B), 077.D-0395(C), and 077.D-0395(D). We wish to thank the ESO staff for the support during these observations, M. Gillon who made available the deconvolution code DECPHOT, and the anonymous referee for his/her suggestions which improved this paper. NR is

supported by a Ramon y Cajal Research Fellowship, and thanks R. Mignani for useful discussion, and E. Keane for his comments on the manuscript. MAM is supported by a WV EPSCoR grant, and a SAO guest investigator grant, and B.M.G. acknowledges the support of the Australian Research Council through grant FF0561298.

## REFERENCES

- Beloborodov, A., & Thompson, C. 2007, *ApJ*, 657, 967
- Briskin, W. F., Thorsett, S. E., Golden, A., Goss, W. M. 2003, *ApJ* 593, L89
- Chatterjee, P., Hernquist, L., & Narayan, R. 2000, *ApJ*, 534
- Camilo, F., Ransom, S. M., Halpern, J. P., Reynolds, J., Helfand, D. J., Zimmerman, N., Sarkissian, J. 2006, *Nature*, 442, 892
- Camilo, F., Ransom, S. M., Halpern, J. P., Reynolds, J. , 2007, *ApJ*, 666, L93
- Caraveo, P. A., Biglami, G. F., Mignani, R., Taff, L. G. 1996, *ApJ*, 461, L91
- Cardelli, J. A., Clayton, G. C., Mathis, J. S. 1989, *ApJ*, 345, 245
- Cordes, J. M. & Shannon, R. M. 2008, 682, 1152
- DeLaney, T., Gaensler, B. M., Arons, J., Pivovarov, M. J. 2006, *ApJ* 640, 929
- Dhillon, V. S., Marsh, T. R. & Littlefair, S. P. 2006, *MNRAS*, 372, 209
- Dodson, R., Legge, D., Reynolds, J. E., McCulloch, P. M. 2003, *ApJ*, 596, 1137
- Eikenberry, S. S., et al. 2004, *ApJ*, 616, 506
- Gaensler, B. M., Brazier, K. T. S., Manchester, R. N., Johnston, S., Green, A. J. 1999, *MNRAS*, 305, 724
- Gaensler, B. M., McClure-Griffiths, N. M., Oey, M. S., Haverkorn, M., Dickey, J. M., Green, A. J. 2005, *ApJ* 620, L95
- Gillon M., Pont F., Moutou C., Bouchy, F., Courbin, F., Sohy, S., Magain, P, 2006, *A&A*, 459, 249
- Gillon M., Magain P., Chantry V., Letawe, G., Sohy, S., Courbin, F., Pont, F., Moutou, C 2007, *ASPC*, 366, 113,
- Haberl, F. 2007, *Ap&SS*, 308, 73
- Hulleman, F., Tennant, A. F., van Kerkwijk, M. H., Kulkarni, S. R., Kouveliotou, C., Patel, S. K. 2001, *ApJ*, 563, L49
- Hulleman, F., van Kerkwijk, M. H., Kulkarni, S. R. 2004, *A&A*, 416, 1037
- Israel, G. L., et al. 2002, *ApJ*, 580, L143
- Israel, G. L., et al. 2003, *ApJ*, 589, L93
- Israel, G. L., et al. 2004, *IAUS* 218, 247
- Israel, G. L., et al. 2005, *A&A* 438, L1
- Israel, G. L., et al. 2009, *ATel* # 1909
- Kaplan, David L. & Moon, D-S 2006, 644, 1056
- Kaplan, D. L., Esposito, P., Chatterjee, S., Possenti, A., McLaughlin, M. A., Camilo, F., Chakrabarty, D., Slane, P. O. 2009, *MNRAS*, 400, 1445
- Kargaltsev, O. Y., Pavlov, G. G., Zavlin, V. E., Romani, R. W. 2005, *ApJ*, 625, 307
- Keane, E.F. & Kramer, M. 2008, *MNRAS*, 391, 2009
- Keane, E.F., Ludovici, D. A., Eatough, R. P., Kramer, M., Lyne, A. G., McLaughlin, M. A., Stappers, B. W. 2010, *MNRAS* , 401, 1057
- Koptsevich, A. B., Pavlov, G. G., Zharikov, S. V., Sokolov, V. V., Shibanov, Yu. A., Kurt, V. G. 2001, *A&A* 370, 1004
- Kothes, R., Uyaniker, B., Yar, A. 2002, *ApJ*, 576, 169
- Li, X.-D. 2006, *ApJ*, 646, L139
- Lo Curto, G., Mignani, R. P., Perna, R., Israel, G. L. 2007, *A&A*, 473, 539
- Lyne, A., McLaughlin, M. A., Keane, E. F., Kramer, M., Espinoza, C. M., Stappers, B. W., Palliyaguru, N. T., Miller, J. 2009, *MNRAS* 400, 1439
- Luo, Q. & Melrose, D. B. 2007, *MNRAS*, 378, 1481
- Magain P., Courbin F., Gillon M., Sohy, S., Letawe, G., Chantry, V., Letawe, Y. 2007, *A&A*, 461, 373
- Magain P., Courbin F., Sohy, S., 1998, *AJ*, 494, 47
- McLaughlin M. A., et al. 2006, *Nature*, 439, 817
- McLaughlin M. A., et al. 2007, *ApJ*, 670, 1307
- McLaughlin M. A., et al. 2009, *MNRAS*, 400, 1431
- Bibby, J. L., Crowther, P. A., Furness, J. P., Clark, J. S. 2008, *MNRAS* 386, L23
- Mereghetti, S., Tiengo, A., Stella, L., Israel, G. L., Rea, N., Zane, S., Oosterbroek, T. 2004, *ApJ*, 608, 427
- Mereghetti 2008, *2008A&ARv*, 15, 225
- Mignani, R. P., et al. 2001, *A&A*, 376, 213
- Mignani, R. P., De Luca, A., Kargaltsev, O., Pavlov, G. G., Zaghia, S., Caraveo, P. A., Becker, W. 2003, *ApJ*, 594, 419
- Mignani, R. P., Perna, R., Rea, N., Israel, G. L., Mereghetti, S., Lo Curto, G. 2007, *A&A*, 471, 265
- Mignani, R. P. 2009, *arXiv0908.1010*
- Pavlov, G. G., Welty, A. D., Cordova, F. A. 1997, *ApJ* 489, L75
- Pavlov, G. G., Zavlin, V. E., Sanwal, D., Burwitz, V., Garmire, G. P., 2001, *ApJ* 552, L129
- Popov, S. 2006, *MNRAS*, 369, L23
- Predehl, P. & Schmitt, J.H.M.M. 1995, *A&A* 293, 889
- Rea, N., et al. 2004, *A&A* 425, L5
- Rea, N., et al. 2007, *MNRAS*, 381, 293
- Rea, N. & McLaughlin, M. A. 2008, *AIP Conference Proceedings*, 968, 151
- Rea, N., Zane, S., Turolla, R., Lyutikov, M., Götz, D. 2008, *ApJ*, 686, 1245
- Rea, N., et al. 2009a, *ApJ*, 703, L41
- Rea, N., et al. 2009b, *MNRAS*, 396, 2419
- Reynolds, S. P., et al. 2006, *ApJ*, 639, L71
- Shearer, A., et al. 1997, *ApJ*, 487, L75
- Shibanov, Yu. A., Koptsevich, A. B., Sollerman, J., Lundqvist, P. 2003, *A&A*, 406, 645
- Sollerman, J., Lundqvist, P., Lindler, D., Chevalier, R. A.; Fransson, C., Gull, T. R., Pun, C. S. J.; Sonneborn, G. 2000, *ApJ*, 537, 861
- Sollerman, J. 2003, *A&A*, 406, 639
- Testa, V., et al. 2008, *A&A*, 482, 607
- Tian, W. W., Leahy, D. A., & Li, D. 2010, *MNRAS*, 404, L1
- Wang, Z. & Chakrabarty, D. 2002, *ApJ*, 579, L33
- Weisskopf, M. C., et al. 2000, *ApJ* 536, L81
- Weltevrede, P., Stappers, B., Rankin, J., Wright, G. 2006, *ApJ*, 645, L149
- Woods, P. M., et al. 2004, *ApJ*, 605, 378
- van Kerkwijk, M. H. & Kaplan, D. L., 2007, *Ap&SS*, 308, 191
- Zane, S., Mignani, R. P., Turolla, R., Treves, A., Haberl, F., Motch, C., Zampieri, L., Cropper, M. 2008, *ApJ*, 682, 487
- Zhang, B., Gil, J., & Dyks, J. 2007, *MNRAS*, 374, 1103
- Zharikov, S.V., Mennickent, R. E., Shibanov, Yu., Komarova, V. 2007, *Ap&SS*, 308, 545